Review
Mathematical description of the mechanical behaviour of metallic materials under creep conditions

N. D. BATSOULAS
Mechanical Engineering Department, School of Engineering, University of Patras, Patras, Greece

The metallic materials creep behaviour has been described and a complete model is presented. The basic constitutive equation, as well as the structure parameters, have been derived from a mathematical analysis that represents the dominant physical procedures and mechanisms. The model is very general because it is referred to all stages of creep and describes the creep behaviour of all metallic materials, including those strengthened by a dispersion of second-phase particles. A creep function has been derived from the constitutive equation describing all three stages of creep under constant loading. The function has the minimum possible number of fitting, parameters. The dependence of the fitting parameters on the loading conditions has been described using very simple mathematical relations. Applications and predictions have been carried out in a wide range of metallic materials. Good agreement has been shown by a comparison made also between the creep curves determined experimentally, and those obtained from creep function and determined fitting parameters.

1. Introduction

The complication of metallic materials mechanical behaviour under creep conditions has had, as a consequence, the absence, until now, of a model leading to generally accepted constitutive equations. Partial attempts have been made, converging to a common goal which still remains unaccomplished. On the other hand, the need remains for valid constitutive equations to satisfy the design requirements.

The principle that the equations are more valid when they are based on actual physical procedures is generally accepted today. This principle constitutes a very strong motive for utilizing knowledge of the nature of creep deformation in the structural composition of models leading to constitutive equations. This is the modern trend for the mathematical modelling which is replacing the older trend for the development of constitutive equations which was exclusively based on experiment. Knowledge of the role of the internal structure (for example, dislocation density, cavity density) for the response of the non-elastic deformation is critical. This leads to the use of state variables (structure parameters) for the prediction of the transient and steady-state response.

In general, there are three types of model producing constitutive equations: physical (microscopic), phenomenological (macroscopic, empirical) and physical–phenomenological (micro-macroscopic). The basic elements for the formulation of the physical models are relations concerning the particular elementary physical procedures while the variables in these relations are real physical quantities, for example, atomic volume, etc. Of course these physical quantities are assembled to construct more complicated structures but the distinctive difference is that there always exists a separate representation of the actual physical quantities. It is obvious that the physical models cannot lead to general constitutive equations. Moreover, even if the physical models did lead to general constitutive equations, the very large number of parameters, many of which would not have a value, would render them useless for applications. To start with, it is accepted that, in the physical–phenomenological models, the physical procedures defining the behaviour to be modelled are too complicated to be represented in terms of actual physical quantities. However, on the other hand, it is acknowledged that there is sufficient scientific knowledge of the physical mechanisms in order to understand adequately the main mechanism controlling the behaviour. Therefore, after an analysis, state variables (structure parameters) corresponding to the dominant physical procedures can be produced and equations of state variables can be formulated, so that the behaviour of the state variables simulates the behaviour of the physical variables under the same conditions. Therefore, there is a one to one correspondence between the transient response of the constitutive variables in the physical–phenomenological

model and the actual behaviour of the physical quantities in the real material. This is the distinctive difference between a physical–phenomenological model and a simple fitting to macroscopic data, or to an expanded form of them.

Certainly, a complete model requires not only a correct selection of state variables and accurate formulae (with proper mathematical processing) for the equations that associate the variables, but also special algebraic expressions for the dependencies of the various fitting parameters on the straining quantities. This state of development includes the procedure of fitting to experimental data for the derivation of the best expression. It should be emphasized that one of the main criteria for the evaluation of the various models is the number of fitting parameters which should remain as small as possible, without, though, deviating from the above-mentioned principles.

In earlier work [1–6], basic conclusions were formulated that led to effective partial applications for the metallic materials creep under various straining conditions. In the present paper, a general physical–phenomenological model for the creep of metallic materials, including those strengthened with second-phases particles, is formulated and fully justified. The analytical mathematical presentation of the model is performed and an effective creep function with the minimum possible number of fitting parameters is presented. That is, the all theoretical analysis results in a useful tool for mechanical design.

2. Initial and secondary creep
2.1. Fundamental concepts and main mechanisms

The common ground of all dislocation creep theories is the knowledge that the material is hardened with the deformation and is softened with time (while heated). These two procedures take place simultaneously and define the strain. This idea was first formulated by Bailey and Orowan [7] and was successively developed by a large number of scientists. At a high temperature, usually about the one-third of the absolute melting temperature, the dislocations acquire a new degree of freedom. Except for gliding, there is also climbing, and therefore the dislocations are not obliged to move only on their slip planes. This results in the gradual release of dislocations previously created with the strain. The structure of the dislocations is subjected to the so-called recovery. This means that if a dislocation is held by an obstacle, the recovery procedure will release it, allow it to slide down to the next obstacle, the glide step of the dislocation being responsible for almost the total strain. The mechanisms which are based on this succession of glide–climb of dislocations are referred to as hardening-recovery mechanisms. The characteristic difference which distinguishes these mechanisms from those of plastic flow under lower temperatures (which mechanisms may also be thermally activated) is that the procedure, at an atomic level, is rather the diffusive movement of the atomic voids towards or from the dislocation, which glides more, than the gliding of the

dislocation as a whole [8]. The modern unified way of describing the gliding phenomena and of dislocation hardening and recovery, is the theory of a dislocations network and of an internal back stress [9–19].

In accordance with the experimental observations, it has been assumed that the dislocations are arranged to form a network. The creep procedure consists of continuous events of recovery and hardening. The coherence of the network is ensured by the repulsive and attractive forces among the dislocations. As a result of the applied stress and of the thermal fluctuation, some of the dislocations will escape from the network and will slide a certain distance down to the point where they encounter some obstacle (dislocation, second-phase particle, etc.). During their movement the strain and hardening increase because the dislocations subjected to stress, increase their length and, therefore, their density. The recovery procedure takes place simultaneously. The force for the creep of the dislocations results from the linear stress of the dislocations which have been bent by the obstacles. After the climbing, the procedure is repeated.

At the beginning of the loading (initial creep), many of the dislocations loosely connected to the network will move, and therefore the creep rate will, initially, be very high. But the number of easily escaping dislocations decreases, gradually, with time. This results in the fact that the creep strain increases with a diminishing rate. At this stage, the hardening is dominant and the dislocation density increases. However, the recovery trend increases with the increase in the dislocation density, therefore, the recovery rate increases and finally, a situation results where the two procedures balance one another while the dislocation density and the creep rate remain constant (secondary creep). The time required for a dislocation to overcome an obstacle has to do with the flow of atomic voids at jogs of its length. What is characteristic is that the higher the stress and the temperature, the faster is the climb. The time required for a dislocation to slide depends on the relationship between the applied stress and the stress coming from the dislocations network (elastic dislocation field). Dissolved atoms (foreign atoms) which are attracted to the elastic dislocation field and which attempt to be diffused while the dislocation slides, create a friction force with the lattice and can decelerate its movement. In a material that was strengthened with second-phase particles and the ratio of the particles volume with respect the total volume is large enough, the opposing stress consists of a component that is due to the particles [20].

The model of a dislocation sliding on the sliding plane is represented by a load sliding on a plane, σ_f is the friction stress in the lattice during the movement of the dislocation because of foreign (interstitial) atoms. σ_p is the internal stress of particles coming from the elastic field of the distributed second-phase particles. The stress that is applied on the dislocation and that is due to the network of the rest dislocations, is called the internal back stress and is represented by the symbol σ_i. In general, it can be assumed that $\sigma_f \cong 0$ when the atomic size of the interstitial atoms is not considerably different from that of the lattice atoms,

while σ_p is taken into account only in metallic materials heavily hardened with particles. In order for strain to take place, the dislocation has to glide under the applied external stress which is herein represented by σ. If $\sigma \leqslant \sigma_i$, glide will not take place for a limited period of time until the internal back stress is self-adjusted to new values. The above formulation does not include existing inelastic phenomena related to the grain boundary. But as shown in a previous study [11], these phenomena can be neglected. At the microscopic scale, the hardening is controlled by the rate at which the dislocations approach each other, while the recovery takes place through rearrangement (and counterbalancing) of the dislocations. Therefore, the applied stress is composed of two terms: the mean internal back stress, which is related to the recovery–hardening equilibrium, and the mean effective stress that is responsible for the glide [21, 22]. The concept of the mean internal back stress (and, respectively, of the mean effective stress) has been proven to be a very important phenomenological structure parameter because it is directly related to the dominant procedure of dislocations movement.

2.2. Analytical processing and basic relations

Consider L as the free dislocation length, that is length between two obstacles (dislocation link length). L is the possible elementary glide unit and, at the same time, the element forming the dislocations network. The variable L is of stochastic character [23–26]; let N be the probability density function of distribution L. Using L as a weights variable, the mean internal back stress, σ_i, can be written as

$$\sigma_i = \frac{\int_{\hat{L}} \sigma_i' N L \mathrm{d}L}{\int_{\hat{L}} N L \mathrm{d}L} \tag{1}$$

where $\hat{L}$ is the range of L and σ_i' the local internal back stress. The local internal stress can be written as a function of L [27–29]

$$\sigma_i' = \frac{a' G b}{L} \tag{2}$$

where G is the shear modulus, b Burgers' vector and a' is a numerical coefficient. If Λ is the mean dislocation length, that is $\Lambda = \bar{L}$, then Equations 1 and 2 lead to

$$\sigma_i = \frac{a' G b}{\Lambda} \tag{3}$$

The mean dislocation length, Λ, is related to the (mean) dislocation density, ρ. Dislocation density is defined as the total dislocation length per unit of volume or, alternatively, the number of dislocations passing through a unit cross-section. On the basis of the above symbolizations one can write

$$\rho = \frac{\int_{\hat{L}} L N \mathrm{d}L}{V} \tag{4}$$

where V is the volume of the considered crystal. Assuming that volume V is cut to polyhedra, the sides and the edges of which constitute the loops and the nodes of the network, respectively [30, 31], then the volume can be estimated as follows

$$V = M_g \Lambda \int_{\hat{L}} L^2 N \mathrm{d}L \tag{5}$$

where M_g is a geometric term. Equations 4 and 5 lead to

$$\rho = \frac{\Lambda}{M_g \Lambda (\overline{L^2})} \tag{6}$$

If σ_k is the standard deviation of the distribution, then

$$(\overline{L^2}) = M_k \Lambda^2 \tag{7}$$

where

$$M_k = 1 + \left(\frac{\sigma_k}{\Lambda}\right)^2$$

From the above equation, it results that the coefficient, M_k, may be practically considered independent of the structure of the dislocations network. Equations 6 and 7 lead to

$$\Lambda = (M_g M_k \rho)^{-1/2} \tag{8}$$

Equations 3 and 8 lead to

$$\sigma_i = \frac{(abG)^2}{2} \frac{\dot{\rho}}{\dot{\sigma}_i} \tag{9}$$

where $\quad a = a' (M_g M_k)^{1/2}$

Hereafter the mean internal back stress, σ_i, will be referred to as, simply, internal stress, σ_i. The above relation results in the independence of the coefficient a of the network's structure. The dot means a time derivative.

From the basic Orowan's relation the dependence of the creep rate on the density of the moving dislocations, ρ_m, can be derived [32, 33]

$$\dot{\varepsilon}^c = M_T \rho_m b v$$

where v is the mean dislocation's velocity and M_T is Taylor's numerical coefficient. The very important fact that this relation is also valid for the initial creep [10, 11] should be emphasized. From Section 2.1, the high internal stresses are seen to correspond to a small ratio of moving dislocations, while a very high ratio of moving dislocations corresponds to low internal stresses. Therefore, ρ_m is a function of σ_i and, of course, of the applied stress because of its relation with the hardening. As a result it can be written that $\rho_m = \rho_m(\sigma, \sigma_i)$. According again to the analysis of Section 2.1, the mean dislocations velocity is a function of the effective stress, σ_e, and, of course, of the temperature because of its relation to the dislocations climb which is thermally controlled. Therefore, $v = (\sigma_e, T)$. Consequently, Orowan's equation can be written

$$\dot{\varepsilon}^c = M_T b \rho_m(\sigma, \sigma_i) v(\sigma_e, T) \tag{10}$$

The following relation has been suggested for the function ρ_m [11, 18, 19]

$$\rho_m = \rho_0(\sigma) \sigma_i^{\xi_1} \tag{11}$$

For the function v, the following relation has been suggested [9, 11, 18]

$$v = v_0(T)\,\sigma_e^{\xi_2} \tag{12}$$

where ρ_0, v_0, ξ_1 and ξ_2 are constants.

Ahlquist and Nix [11], gave the following approximations for the exponents: $\xi_1 = -1$, $\xi_2 = +1$. Therefore Equations 10 results in the following relation

$$\dot{\varepsilon}^c = M_T b \rho_0 v_0 \frac{\sigma_e}{\sigma_i} \tag{13}$$

If we insert Equation 9 into Equation 13 then

$$\sigma_e = \frac{b(aG)^2}{2M_T \rho_0 v_0} \frac{\dot{\rho}}{\sigma_i} \dot{\varepsilon}^c \tag{14}$$

From Section 2.1 the following fundamental relation can be derived

$$\sigma = \sigma_i + \sigma_e \tag{15}$$

therefore Equations 9 and 14 result in

$$\sigma = \frac{(abG)^2}{2} \frac{\dot{\rho}}{\dot{\sigma}_i} + \frac{b(aG)^2}{2M_T \rho_0 v_0} \frac{\dot{\rho}}{\dot{\sigma}_i} \dot{\varepsilon}^c \tag{16}$$

The change in the dislocation density, as already mentioned, is considered to consist of two terms of hardening and recovery

$$d\rho = (d\rho)_1 - (d\rho)_2 \tag{17}$$

The first term essentially describes a change in the dislocations – obstacles density that is due to the fact that a specific ratio of the moving dislocations density, ρ_m, was immobilized in the crystal after it started to move over a distance dx. This term can be written as follows [34]

$$d\rho_1 = \rho_m \frac{dx}{\Lambda} \tag{18}$$

The second contribution to the change of the dislocation density is due to a certain recovery or rearrangement procedure which takes place among dislocations previously started.

The number of possible recovery locations on an elementary surface, ds, of the sliding plane is ρds. When a mean length, Λ_r, of the dislocation is counterbalanced or is, in another way, rendered inactive, the total change in the dislocation length in the volume, V, at every possible recovery location, is

$$V(d\rho)_2 = \Lambda_r \rho ds \tag{19}$$

Given a crystal of thickness, h, that contains a dislocation, then the shear strain, $d\gamma$, can be written as

$$d\gamma = \frac{b}{h}$$
$$= \rho_m b dx$$
$$= \frac{b ds}{V} \tag{20}$$

Combining Equations 17–20 and taking into account Equation 8 we obtain

$$\frac{d\rho}{d\gamma} = \frac{M_g M_k}{b} \rho^{1/2} - \frac{\Lambda_r}{b} \rho \tag{21}$$

As far as the axial strain, ε^c, is concerned, the above relation can be written as

$$\frac{d\rho}{d\varepsilon^c} = k_1 \rho^{1/2} - k_2 \rho \tag{22}$$

where the abbreviations $k_1 = \alpha'(M_g M_k)^{1/2}/b$, $k_2 = \alpha'\Lambda_r/b$, are used. α' is a numerical coefficient.

With the transformation $R = \rho^{1/2}$, Equation 22 leads to

$$\frac{dR}{d\varepsilon^c} = \frac{k_1}{2}\left(1 - \frac{Rk_2}{k_1}\right) \tag{23}$$

Function $R(\varepsilon^c)$ presents a stationary point at the value $R = R_S$ where $dR/d\varepsilon^c = 0$. Also for $\varepsilon^c = \varepsilon_0^c = 0$, it can be considered that $R = R_0$. Therefore:

$$\rho = R_S^2 - [2R_S(R_S - R_0)\,e^{-(k_2/2)\varepsilon^c} - (R_S - R_0)^2\,e^{-(k_2/2)\varepsilon^c}] \tag{24}$$

Considering that it can be written that:

$$x_1 e^{y_1} - x_2 e^{y_2} \cong (x_1 - x_2)e^{(x_1 y_1 - x_2 y_2)/(x_1 - x_2)}$$

Equation 24 is transformed to

$$\rho = R_S^2 - (R_S^2 - R_0^2)\,e^{-[R_0 k_2/(R_S + R_0)]\varepsilon^c} \tag{25}$$

Hereafter, ε^c in the exponent is represented as $\varphi(t)$.

For the unknown function $\varphi(t)$, the following data are known from experiments:

(i) $\varphi(t)$ is continuous, properly increasing and positive,

(ii) its derivative $\varphi_0(t)$ is continuous and presents a minimum $\varphi_0(\varphi_0 > 0)$, and that

(iii) $\varphi(0) = 0$

Therefore

$$\dot{\rho} = R_0(R_S - R_0)k_2 \varphi_0(t)\,e^{-[R_0 k_2/(R_S + R_0)]\varphi(t)} \tag{26}$$

Taking into account Equation 26, the differential Equation 16 takes the form

$$\sigma = A \frac{\varphi_0(t)}{\dot{\sigma}_i}\,e^{-c\varphi(t)} + B \frac{\varphi_0(t)}{\dot{\sigma}_i}\,e^{-c\varphi(t)}\dot{\varepsilon}^c \tag{27}$$

where the abbreviations

$$A = \frac{(abG)^2}{2} R_0(R_S - R_0)k_2 \tag{27a}$$

$$B = \frac{b(aG)^2}{2M_T \rho_0 v_0} R_0(R_S - R_0)k_2 \tag{27b}$$

$$c = \frac{R_0 k_2}{R_S + R_0} \tag{27c}$$

are used. The above relations imply that: A, B, $c > 0$.

We consider the differential equation

$$\dot{\varepsilon}^c = \frac{A\varphi_0(t)\,e^{-c\varphi(t)} - Ce^{-\beta t}\varepsilon^c}{De^{-\beta t} - B\varphi_0(t)e^{-c\varphi(t)}} = f(t, \varepsilon^c) \tag{28}$$

where C, D and β are non-negative coefficients. The differential Equation 28, together with the condition $\varepsilon^c(0) = 0$, constitutes an initial-value problem. $f(t, \varepsilon^c)$ is a function of two variables and is defined in the domain Δ such that $t \geqslant 0$, $\varepsilon^c \geqslant 0$. For the function

$f(t, \varepsilon^c)$ for every ε_1^c ε_2^c, the following is valid

$$|f(t, \varepsilon_1^c) - f(t, \varepsilon_2^c)| = \frac{C|\varepsilon_1^c - \varepsilon_2^c|}{|D - B\varphi_0(t) e^{\beta t - c\varphi(t)}|} \quad (29)$$

where $C > 0$. There is β with $\beta > 0$ such that $\beta t > c\varphi(t)$ for every t. Therefore

$$B\varphi_0(t) e^{\beta t - c\varphi(t)} - D > B\varphi_0 - D$$

For $0 < D < B\varphi_0$ (this inequality is compatible with inequality $D < B\varphi_0(0)$ that results from Equation 28. The case $D = 0$ is rejected because it results in $\varepsilon^c(0) < 0$,

$$\frac{1}{|B\varphi_0(t) e^{\beta t - c\varphi(t)} - D|} < \frac{1}{B\varphi_0 - D}$$

As a result, Equation 29 takes the form

$$|f(t, \varepsilon_1^c) - f(t, \varepsilon_2^c)| < \lambda |\varepsilon_1^c - \varepsilon_2^c| \quad (30)$$

where

$$\lambda = \frac{C}{B\varphi_0 - D} > 0$$

Therefore, with the constraints already mentioned for the coefficients C, D and β, the function $f(t, \varepsilon^c)$ is a Lipsitz function [35, 36] with λ as a constant. Moreover, it is bounded. In fact, for function $f(t, \varepsilon^c)$ the following is valid

$$|f(t, \varepsilon^c)| < \frac{[C/\varphi_0(t)] e^{-\beta t + c\varphi(t)} \varepsilon^c + A}{|[D/\varphi_0(t)] e^{-\beta t + c\varphi(t)} - B|} \quad (31)$$

However

$$\left| \frac{D}{\varphi_0(t)} e^{-\beta t + c\varphi(t)} - B \right|^{-1} < \left| \frac{D}{\varphi_0} - B \right|^{-1}$$

Also with the stronger constraint $\beta t > (c + 1)\varphi(t)$, for every t, it is derived that

$$\frac{C}{\varphi_0(t)} e^{-\beta t + c\varphi(t)} \varepsilon^c < \frac{C}{\varphi_0}$$

As a result, Inequality 31 takes the form

$$|f(t, \varepsilon^c)| < M_f \quad (32)$$

where

$$M_f = \frac{C + A\varphi_0}{B\varphi_0 - D} > 0$$

That is, M_f is a bound of $f(t, \varepsilon^c)$ in the domain Δ.

The conditions of Emile Picard's theory are fulfilled [35, 36], and therefore the initial-value problem (Equation 28) has one and only one solution for $t \geq 0$. That is, it has been shown that there are C, D and β such as that Equation 28 is valid for every $t \geq 0$. Equations 27 and 28 lead to

$$\sigma = C \frac{e^{-\beta t}}{\dot{\sigma}_i} \varepsilon^c + D \frac{e^{-\beta t}}{\dot{\sigma}_i} \dot{\varepsilon}^c \quad (33)$$

3. Tertiary creep
3.1. Metallic materials creep failure mechanisms
The creep acceleration at the third stage is due to the creation and joining of cavities at the boundaries of grains, that is, the fracture in creep is, generally, inter-crystalline. The cavities may be created at the beginning of creep, even in the first stage. Initially, their effect on the strain rate is negligible but, as their number and size increase, this effect becomes definitive. The accelerating rate of creep can also be caused by the collapse of the materials microstructure. Many metallic materials contain second-phase particles that act as obstacles in the movement of dislocations and improve the strength to creep. Under a straining over a long period of time the possible growth of the larger of these particles and the disappearance of the smaller, leads to increasing rates of creep. But Dyson and McLean showed [37] that, even in nickel superalloys (with a large number of particles), the tertiary creep cannot be explained by the development of particles. The main part of the accelerating rate of creep should be attributed to the cavities of the grain boundary. Another possible cause (not definite) for the accelerating rates of the third stage of creep is the corrosion on or below the surface, as, for example, the internal oxidation (mainly at the boundary grain) and the following creation of a crack.

Under relatively medium stresses and high temperatures the metallic materials are broken with a relatively low ductility. The decrease is due to the inter-crystalline development of cavities. Isolated cavities have been tracked at the second stage of creep and, in some cases, at the first stage. At the later stage, the voids start to become unified at the sides of the grain boundaries, forming small cracks (microcracks). The unification of the microcracks leads to the characteristic fibrous–porous surface of the intercrystalline fracture. The general cause of the transition from the intracrystalline failure (under low temperatures) to the intercrystalline failure is that the atomic voids are rendered agile under high temperatures. The atomic voids that are dispersed at the boundaries of grains can be concentrated to form cavity nuclei. Moreover, the grain boundaries are active sources of voids so that they supply the creation of cavities. In the alloys that usually contain second-phase particles at the limits of grains, the cavities are, usually, created at the place of the particles. Numerous studies have shown that in the low alloyed steels, the austenitic steels as well as the nickel superalloys, the cavities are related to carbides, as well as to sulfides, silicates and oxides existing in the main material.

The development of creep damage can be expressed in terms of two mechanisms [38–40]. The one mechanism is the creation of cavities and provides a measure for the rate at which the number of voids increases and the other mechanism has to do with the development of cavities and provides a measure of the magnification of cavities with time. The rate of creation of voids is represented as $\dot{M}$ and is measured with the number of cavities created per unit of time on the unit area of the grain's boundary. Let $\dot{M}(\xi)$ be the rate of creation of cavities in a time ξ. Therefore, in the time interval $d\xi$, the number of new cavities created is $\dot{M}(\xi)d\xi$. In the later time, t, these cavities will be magnified and the assumed rate of development of the cross-sectional area of the cavities created in time ξ will be $\dot{W}(t, \xi)$.

The total area, S, of the voids in time t_f is therefore

$$\frac{S}{S_0} = \int_0^{t_f} \dot{M}(\xi) \mathrm{d}\xi \int_\xi^{t_f} \dot{W}(t, \xi) \mathrm{d}$$

where S_0 is the total cross-section. The above formulation is general but shows that, in order to define a measure of damage, the effect of both functions M and W should necessarily be known.

Rabotnov and Kachanov [41], simplifying the analysis at this point, considered the ratio $\omega = S/S_0$ as a phenomenological (state) variable, and used the condition $\omega = 1$ as the failure condition. They assumed that the following relation is valid

$$\frac{\mathrm{d}\omega}{\mathrm{d}t} = \hat{B} \frac{\sigma^{\hat{k}}}{(1 - \omega)^{\hat{k}}} \qquad (34)$$

where $\hat{k}$ is a constant. Moreover, similar relations have been proposed for the development of damage [42, 43].

It is important to emphasize that, using the effect of damage on the tertiary creep, it is possible to measure the quantity ω. In fact, in other studies [44, 45], a method of measuring ω is suggested. Moreover, Equation 34 is in perfect accordance with the experimental data. Therefore, the variable ω concept is a fully defined macroscopic structure parameter.

3.2. The effect of damage on the rate of creep

An obvious mechanism by which the intercrystalline cavities can increase the creep strain rate is the decrease in the effective cross-section that bears the load and therefore the increase in the essential stress at the effective cross-section [41, 46, 47]. Another mechanism, which sometimes may be important, is the increase in the volume of the specimen because of the cavities, which also has a specific contribution to the strain. Moreover, the loss in the effective cross-section is not large enough to explain fully the increasing strain rate. Nevertheless, it has been proved that the tertiary creep is related to the creation of cavities. The following idea has been proposed as a satisfactory explanation. The recovery is quicker in the presence of cavities because these may act as a particularly capable sink of atomic voids and therefore, they may promote the dislocation climb procedure [18, 48, 49]. Using the concept of damage ω, Equation 33 can be modified so that it takes into account both the decrease in the cross-section and the acceleration of the recovery procedure. This can be realized by the replacement of σ by $\sigma/(1 - \omega)$ and of σ_i by $(1 - \omega)^r \sigma_i$, where r is a numerical coefficient. The result is

$$\frac{\sigma}{1 - \omega} = C \frac{e^{-\beta t}}{(1 - \omega)^{1-r} \dot{\sigma}_i} \varepsilon^c + D \frac{e^{-\beta t}}{(1 - \omega)^{1-r} \dot{\sigma}_i} \dot{\varepsilon}^c \qquad (35)$$

4. The basic constitutive equation

Equation 35 is transformed to

$$\sigma = C \frac{e^{-\beta t}(1 - \omega)^r}{\dot{\sigma}_i} \varepsilon^c + D \frac{e^{-\beta t}(1 - \omega)^r}{\dot{\sigma}_i} \dot{\varepsilon}^c \qquad (36)$$

Equation 36 constitues a generalization of Equation 33 applied also to the third stage in so far as of the first and second stage, the damage although it exists, it can be neglected ($\omega \to 0$) as already mentioned. The literature supports the validity of Equation 36 in many different ways. For example, in order to take into account the material's damage [50, 51], the following generalized equation was proposed for the case of creep

$$\sigma = \Psi_0(.) Z \varepsilon^c + \Psi_1(.) \zeta \dot{\varepsilon}^c \qquad (37)$$

Z and ζ are functions capable of describing the creep behaviour without damage, while $\Psi_0(.)$ and $\Psi_1(.)$ are generalized damage functions that are properly selected. The above relation is evidently compatible with Equation 36 but is of phenomenological origin and is arbitrarily formulated. Moreover in a previous study [52], measurements were formulated and performed at different times for the number, size and total volume of cavities. In addition, in this microscopic point of view, the resultant relations are compatible with Equation 36.

The basic conclusion derived both from Equation 36 and from analysis of Section 1 is that, in order to describe the entire creep curve, two structure parameters are required, $X_1 = \dot{\sigma}_i$ and $X_2 = \omega$ that correspond to the dominant procedures of the dislocation movement and the development of cavities.

The fundamental Equation 36 is also valid for the metallic materials that are heavily hardened with second-phase particles. This important conclusion is derived after taking into account the effect of internal stress of particles σ_p. In fact, as follows from Section 2.1, for this particular case, Equation 15 takes the form

$$\sigma = \sigma_p + \sigma_i + \sigma_e \qquad (38)$$

Equation 8, expressing the fact that the mean free length of dislocations, Λ, is proportional to $\rho^{-1/2}$ should be abandoned when the distance between the obstacles of the dislocations, which defines the mean free length, is a geometrically defined quantity [53]. This is the case in the presence of an exceptional number of particles (separated by a distance smaller than a critical value) or of very fine-grained materials, where the mean free length is defined by the distance between the particles or the size of the grains, respectively. Therefore, the term describing the hardening in Equation 22 becomes constant and the equation takes the form

$$\frac{\mathrm{d}\rho}{\mathrm{d}\varepsilon^c} = k_3 - k_2 \rho \qquad (39)$$

where the constant k_3 is a function of the mean distance of obstacles. With the conditions $\varepsilon^c = \varepsilon_0^c = 0$ and $\rho = \rho_0$, it is derived that

$$\rho = \frac{k_3}{k_2} - \left(\frac{k_3}{k_2} - \rho_0\right) e^{-k_2 \varepsilon^c} \qquad (40)$$

Equation 40 has exactly the same form as Equation 25. If Equation 38 takes the form

$$\sigma - \sigma_p = \sigma_i + \sigma_e$$

then, exactly the same analysis that was included between Equations 26–32 can be repeated. Then, the following relations result

$$\sigma - \sigma_p = \hat{C} \frac{e^{-\beta t}}{\dot{\sigma}_i} \varepsilon^c + \hat{D} \frac{e^{-\beta t}}{\dot{\sigma}_i} \dot{\varepsilon}^c \qquad (41)$$

But for the internal stress of particles, σ_p, it was found that this is proportional to the applied stress [54]

$$\sigma_p = K_p \sigma \qquad (42)$$

where K_p is a constant and $0 < K_p < 1$. Equations 41 and 42 result in

$$\sigma = \frac{\hat{C}}{1 - K_p} \frac{e^{-\beta t}}{\dot{\sigma}_i} \varepsilon^c + \frac{D}{1 - K_p} \frac{e^{-\beta t}}{\dot{\sigma}_i} \dot{\varepsilon}^c \qquad (43)$$

For the abbreviations $C = \hat{C}/(1 - K_p)$, $D = \hat{D}/(1 - K_p)$, $\hat{\beta} = \beta$, the above equation coincides with Equation 33. This conclusion allows for no particular distinction being made for this type of material in the following analysis, given the fact that the damage procedure, as already shown in Section 3.1, is common to all metallic materials.

Using relations that were previously explained, expressions that approximate representations $\dot{\sigma}_i$ and ω can be provided, so Equations 3 and 8 lead to

$$\sigma_i = aGb\rho^{1/2} \qquad (44)$$

From the above equation and Equation 22 it is derived that

$$\frac{d\sigma_i}{d\varepsilon^c} = \frac{aGbk_1}{2}\left(1 - \frac{k_2 \sigma_i}{aGbk_1}\right) \qquad (45)$$

It is derived from Equation 45 that $\sigma_i(\varepsilon^c)$ takes a value σ_{is} of steady state where $d\sigma_i/d\varepsilon^c$ is zero. Also for $\varepsilon^c = \varepsilon_0^c = 0$, it is considered that $\sigma_i = \sigma_{i0}$. As a result

$$\sigma_i = \sigma_{is} - (\sigma_{is} - \sigma_{i0})e^{-k_2/2(\varepsilon^c - \varepsilon_0^c)} \qquad (46)$$

With the approximation $\varepsilon^c - \varepsilon_0^c \cong \dot{\varepsilon}_0^c\, t$ the relation is transformed to

$$\dot{\sigma}_i = \mu(\sigma_{is} - \sigma_{i0})e^{-\mu t} \qquad (47)$$

where

$$\mu = \frac{k_2}{2}\dot{\varepsilon}_0^c$$

Equation 34 has been considered for the development of damage ω and leads to

$$t_f = \frac{1}{(1 + \hat{k})\,\hat{B}\sigma^{\hat{k}}} \qquad (48)$$

where t_f is the failure time. Therefore, Equation 34 takes the form

$$\frac{d\omega}{dt} = \frac{1}{(\hat{k} + 1)\,t_f(1 - \omega)^{\hat{k}}} \qquad (49)$$

for $t = 0$, $\omega = 0$ as a result

$$(1 - \omega)^r = \left(1 - \frac{t}{t_f}\right)^{r/(\hat{k} + 1)} \qquad (50)$$

For times not very close to the failure, it can be written that

$$(1 - \omega)^r = e^{-\delta t} \qquad (50a)$$

where

$$\delta = \frac{r}{t_f(\hat{k} + 1)}$$

Equations 36, 47 and 50a lead to

$$\sigma = Ke^{-\alpha t}\varepsilon^c + \eta e^{-\alpha t}\dot{\varepsilon}^c \qquad (51)$$

where

$$K = \frac{C}{\mu(\sigma_{is} - \sigma_{i0})} \qquad (51a)$$

$$\eta = \frac{D}{\mu(\sigma_{is} - \sigma_{i0})} \qquad (51b)$$

$$\alpha = \beta - \mu + \delta \qquad (51c)$$

The parameters K, η and α, as derived, are functions of physical quantities and, in the future, they will act as experimentally defined fitting parameters. Also, from the above analysis, $K = K(\sigma, T)$, $\eta = \eta(\sigma, T)$ and $\alpha = \alpha(\sigma, T)$.

After replacing

$$K^*(t) = Ke^{-\alpha t} \qquad (52a)$$

$$\eta^*(t) = \eta e^{-\alpha t} \qquad (52b)$$

Equation 51 takes the final form

$$\sigma = K^*(t)\varepsilon^c + \eta^*(t)\dot{\varepsilon}^c \qquad (53)$$

K^* and η^* are model characteristic parameters.

It has been shown from the analysis that the effect of damage has been incorporated in the fitting parameter α. Therefore, the derived conclusion is that there is a one to one correspondence between $K^*(t)$ and $\eta^*(t)$ and the derivative of the internal stress $\dot{\sigma}_i$ (the only structure parameter left). This basic conclusion was used in the analysis of the response of the time-variable straining [2, 4]. The function of the developed physicophenomenological model is, therefore, complete with the structure parameter $\dot{\sigma}_i$.

5. The creep function
5.1. Previous relations
Because of the long duration of the creep experiments, various relations have been proposed concerning the evolution of strain with time as well as its dependence on the straining conditions. In previous decades, the large volume of theoretical scientific work as well as most of the adopted designing methods were based on the Norton–Bailey relation

$$\dot{\varepsilon} = \sigma^{\hat{n}} \exp\left(-\frac{\hat{Q}}{RT}\right) \qquad (54)$$

where $\hat{n}$, $\hat{Q}$ are material constants, R is the global constant and T the absolute temperature. Nevertheless, the use of this relation in the design means that (i) the creep curve is a straight line, (ii) the initial and tertiary creep are neglected, and (iii) the rate of

secondary creep, $\dot{\varepsilon}_m$ (and the creep life, t_f) is, essentially defined as the exclusive designing parameter. In many cases, this led to the fact that only the secondary creep rate was measured while the rest of creep curve was neglected.

Many problems have been encountered concerning the unsatisfactory nature of the explanations provided for the different values of $\hat{n}$ and $\hat{Q}$ at various stress and temperature ranges. Moreover, the use of Equation 54 in the best case, leads to only one approximate representation of the material's behaviour for designing elements that operate under high temperatures. From the complex form of the creep curves, it is obvious that the procedures for determining $\dot{\varepsilon}_m$ (and t_f), alone, neglect a considerable amount of information on the material behaviour. The change in the values of $\hat{n}$ and $\hat{Q}$ has been explained, up to now, through changes in the creep mechanisms. Nevertheless, microscopic studies did not reveal important changes in the mechanisms such as to justify these irregular changes and the absence of continuous functions $\hat{n}(\sigma, T)$, $\hat{Q}(\sigma, T)$ [55, 56]. The studies show that the secondary creep rate (and the failure time), even though they are simple to measure, should not be considered as quantities that fully characterize the metallic material creep behaviour. At the same time, a detailed study of the creep curves showed that it is completely artificial to define a dominant second stage and to refer to the minimum creep rate as the only quantity to which one can reasonably refer.

Besides the above reasons, there are others that make the description of creep by the secondary creep rate inadequate. Many alloys in modern technology have a creep curve strongly dominated by the tertiary creep because of the impediment of dislocations movement in various ways. Therefore, descriptions and constitutive relations that neglect the tertiary creep lead to a complete failure. Moreover, today mathematical difficulties that existed in the past for the manipulation of the non-linear relations and which, in many times were prohibitive of the design, no longer exist. It is derived from the above analysis that there is a necessity of relations describing the entire creep curve and producing all the useful parameters that will constitute the basis for the development of a complete constitutive relation describing the metallic material creep. Despite the intensive use of Equation 54, early attempts have been made to achieve a complete analytical mathematical description of the metallic materials creep curve. These attempts are also related to the concerns already expressed. A certain number of these relations are presented below. A disadvantage of these relations is their fractional character; that is, the fact that they refer to one or two stages of creep and not to the entire curve. For the first and the second stage. the following relations were suggested.

Andrade's relation [57, 58]

$$\varepsilon = \exp\left[\ln(1 + \varepsilon_0) + \ln(1 + Z_1 t)^{1/3} + Z_2 t\right] - 1 \tag{55}$$

Bhattacharya's relation [59]

$$\varepsilon = \varepsilon_0 + e^{Z_1 t^{b_1}} - 1 \tag{56}$$

Cottrel and Aytekin's relation [60]

$$\varepsilon = \varepsilon_0 + Z_1 t^{b_1} + Z_2 t \tag{57}$$

Chevenard's relation [61, 62]

$$\varepsilon = Z_1 \ln(1 + b_1 t) + Z_2 t \tag{58}$$

Johnson and Frost's relation [63]

$$\varepsilon = \varepsilon_0 + Z_1 t^{b_1} + Z_2 t^{b_2} \tag{59}$$

Mott and Nabarro's relation [57, 62]

$$\varepsilon = \varepsilon_0 \left[\ln(1 + Z_1 t)\right]^{2/3} \tag{60}$$

McVetty and Garofalo's relation [57, 61, 64, 65]

$$\varepsilon = \varepsilon_0 + Z_1(1 - e^{-b_1 t}) + Z_2 t \tag{61}$$

McHenry's relation [57]

$$\varepsilon = Z_1(1 - e^{-b_1 t}) + Z_2(1 - e^{-b_2 t}) \tag{62}$$

Odding's relation [57, 66]

$$\varepsilon = \frac{Z_1 t}{1 + Z_2 t} + Z_3 t \tag{63}$$

Phillips's relation [57, 60]

$$\varepsilon = \varepsilon_0 + Z_1 \ln t \tag{64}$$

Schaar's relation [67, 68]

$$\varepsilon = \frac{Z_1 t^{b_1}}{1 - Z_2 Z_1 t^{b_1}} \tag{65}$$

Tapsell and Prosser's relation [61, 62]

$$\varepsilon = Z_1 \ln(1 + Z_2 t) \tag{66}$$

and Wyatt's relation [57, 60, 69]

$$\varepsilon = Z_1 \ln t + Z_2 t^{b_1} \tag{67}$$

The main relations for the metallic material tertiary creep are as follows.

Davies and Dutton's relation [70]

$$\varepsilon = \varepsilon_t + Z_1 t^{4/5} \tag{68}$$

and Davies and Williams' relation [71]

$$\varepsilon = \varepsilon_t + Z_1 e^{b_1 t} \tag{69}$$

where ε is the total strain. The effects of stresses and temperatures are considered to be incorporated in constants Z_i and b_i. But the fact that these relations do not cover the entire creep curve results in the constitutive dependencies on the stress and the temperature not being referred to in the literature, except in very few instances.

Historically, the first relation that was formulated and that describes the entire creep curve was that of Graham and Walles [72]:

$$\varepsilon = \varepsilon_0 + Z_1 t^{-1/3} + Z_2 t + Z_3 t^3 \tag{70}$$

and was, mainly, empirically derived. In the modern attempts of describing the entire creep curve, the θ-projection method [73–80] is the prevailing one and

uses the following relation for creep strain as a basic tool

$$\varepsilon^c = f(\theta, t)$$

$$= \theta_1(1 - e^{-\theta_2 t}) + \theta_3(e^{\theta_4 t} - 1) \qquad (71)$$

The effect of σ and T is incorporated in the fitting parameters θ_i. For the dependencies $\theta_i = \theta_i(\sigma, T)$ simple relations were found, a fact that provides the possibility of performing not only a good fitting to the experimental data but also a good prediction. The method is mainly of empirical origin and its development is closely associated with metallic materials of advanced technology. Some interpretations for Equation 71 were presented *a posteriori* on the basis of physical mechanisms [77, 78].

5.2. The new function

The model's differential equation (Equation 53) leads to the following expression for the creep strain ε^c:

$$\varepsilon^c = \exp\left(-\int \frac{K^*}{\eta^*}\,dt\right)$$

$$\times \left[\int \frac{K^*}{\eta^*} \exp\left(\int \frac{K^*}{\eta^*}\,dt\right) dt + C_\varepsilon\right] \qquad (72)$$

where C_ε is the integration constant. Replacing Equations 52a and 52b for the parameters K^* and η^*, respectively, it is derived, for the case of creep under constant loading that

$$\varepsilon^c = \left\{ C_\varepsilon + \left(\frac{\sigma}{\eta}\right) \frac{1}{\alpha + (K/\eta)} \exp\left[\left(\alpha + \frac{K}{\eta}\right)t\right]\right\}$$

$$\times \exp\left(-\frac{C}{A}\,t\right) \qquad (73)$$

The initial conditions $t = 0$, $\varepsilon_0^c = 0$ results in

$$C_\varepsilon = -\frac{\sigma}{\alpha\eta + K}$$

and, therefore, the creep strain is now expressed as

$$\varepsilon^c = \frac{\sigma\,e^{\alpha t}}{\alpha\eta + K}\left[1 - e^{-(\alpha + K/\eta)t}\right] \qquad (74)$$

The total strain ε is the sum of the instantaneous elastic strain $\varepsilon_i = \sigma/E$ (E is the Young's modulus) and the creep strain ε^c

$$\varepsilon = \frac{\sigma}{E} + \frac{\sigma\,e^{\alpha t}}{\alpha\eta + K}\left[1 - e^{-(\alpha + K/\eta)t}\right] \qquad (75)$$

This leads to the following expression for the strain rate

$$\dot{\varepsilon} = \frac{\sigma K}{(\alpha\eta + K)\eta}\,e^{-(K/\eta)t} + \frac{\sigma\alpha}{\alpha\eta + K}\,e^{\alpha t} \qquad (76)$$

Equation 75 takes the following form

$$\varepsilon = \frac{\sigma}{E} + \frac{\sigma}{\alpha\eta + K}(1 - e^{-(K/\eta)t}) + \frac{\sigma}{\alpha\eta + K}(e^{\alpha t} - 1) \qquad (77)$$

Equations 77 and 71 lead to the fact that the model's creep function (Equation 77) being identical to that of the θ-projection. But there are only three fitting parameters in the model's function (that is K, η and α) while there are four in the θ-projection equation (that is θ_1, θ_2, θ_3 and θ_4) or even five [80].

Moreover, for relatively short time periods, it can be written that $e^{\alpha t} \cong 1 + \alpha t$. The Equation 77 takes the form

$$\varepsilon = \frac{\sigma}{E} + \frac{\sigma}{\alpha\eta + K}(1 - e^{-(K/\eta)t}) + \frac{K\alpha}{\alpha\eta + K}\,t \qquad (78)$$

which is identical to McVetty and Garofalo's relation (Equation 61) for the initial and secondary creep, while for long time periods $e^{-(K/\eta)t} \cong 0$ is valid and Equation 77 takes the form

$$\varepsilon = \frac{\sigma}{E} + \frac{\sigma}{\alpha\eta + K}\,e^{\alpha t} \qquad (79)$$

which is William and Davies' relation (Equation 69) for the main part of tertiary creep.

There is a considerable volume of literature that supports the use of McVetty and Garofalo's equation (Equations 61 or 78) for the initial and secondary creep of a large group of metallic materials. Garofalo [81] published creep data for stainless steel and showed that they are in accordance with Equation 78. Eriksen [82] analysed data for creep of molybdenum with the result that the relation provided reasonable values. The specimens were subjected to thermal recrystallization treatment at 2000 °C and were tested for creep at 1720 °C in vacuum. Moreover, McVetty and Garofalo's equation was verified for the following materials: for aluminium by Sherby *et al.* [83], for a-iron by McLean and Hale [84], for copper by Feltram and Meakin [85], for nickel monocrystals by Parker [86], Raymond and Dorn [87], for nobelium by Brinson and Argent [88] and for platinum by Carrekar [89] with very good results. Moreover, Evans and Wilshire [90] carried out a test for Ca–Al alloys, while Sidey and Wilshire [91] studied Cu–Ni alloys and verified the satisfactory fitting of the relation to the experimental data. Finally, Amin *et al.* [92], suggested McVetty and Garofalo's equation to be a general law for the metallic initial and secondary creep. Moreover, Davies and William's relation (Equation 69 or 79) has also been experimentally verified for the tertiary creep [71].

6. Comparisons with experimental data

In order to test the model and, mainly, in order to determine the dependencies of the fitting parameters K, η, α and to derive, thus, a prediction system, the creep function is compared to the large group of metallic materials. In order to ensure the indisputable validity of the produced constitutive relations, on the one hand, experiments are carried out in the laboratory and, on the other hand, experiments found in the literature from very different sources are used. The experimental data concern a wide range of practical materials: the highly alloyed steel X6 CrNiMo 17 13 at

700 °C [93], the 800 H alloy at 850° [80], the low alloyed steels 10 CrMo 9 10 [93] and 2 1/4 Cr 1Mo [93] at 600 and 550 °C, respectively, aluminium at 210 °C [90] and the nickel-alloy IN-100 at 1000 °C [95, 96]. The chemical compounds, thermal treatment, as well as the Young's modulus of metallic materials, are analytically presented in Tables I and II. The laboratory-derived experimental data concern the steels X8 CrNiMoNb 16 16, X22 CrMoV 12 1 at 700 and 650 °C, respectively, and oxygen-free copper at 405 °C [1 − 6]. As shown in Fig. 1, there is a perfect agreement between the creep function (Equation 75) and the experimental results in the entire range of the above materials. The same agreement is also presented for the materials tested in the laboratory [1–6]. The dependencies of the fitting parameters on the stress are shown in Figs 2–4. Especially in Fig. 2, the dependencies of the fitting parameter, K, on stress, σ, are presented. The dependencies of the fitting parameter, η, on the stress, σ, are presented in Fig. 3, while the dependencies of the fitting parameter, α, on the stress, σ, are shown in Fig. 4.

As it is indisputably derived from all figures, the parameters can be approximated by the following very simple analytical relations for all the materials

$$K = k \exp(-l\sigma) \qquad (80)$$

$$\eta = m \exp(-n\sigma) \qquad (81)$$

$$\alpha = p \exp(q\sigma) \qquad (82)$$

where the values of k, l, m, n, p, q for the various materials and the temperatures are presented in Table III.

The simple Equations 80–82 are in direct contradiction with the anomalous dependence $\hat{n}(\sigma)$ in Equation 54 which, essentially, cannot be analytically formulated. The dependence of K^* and η^* on time for the various stresses is indicated in Figs 5 and 6, respectively. For relatively small loading stresses, where the structure of the material changes slowly with time, the values of K^* and η^* also change slowly, while for high stresses the rapid change in the structure of the material leads to a remarkable change in K^* and η^* with

TABLE I Chemical compositions of the materials. The concentrations of the alloyed elements are given in wt %

Material	C	Si	Mn	P	S	Cr	Mo	V	Mg	Ti	Cu	Zn	Co	Al	Ni	Fe
X 6 CrNiMo 17 17 (DIN 17006)	0.065	0.423	1.62	0.018	0.023	17.06	2.26	0.02	–	–	–	–	–	–	13.32	Bal.
800H (ASTM B163)	0.05–0.10	1.0	–	–	–	19–23	–	–	1.5	0.05–0.10	–	–	–	0.15–0.60	30–35	Bal.
10 CrMo 9 10 (DIN 17006)	0.105	0.24	0.93	0.012	0.014	2.29	1.005	–	–	–	0.09	–	–	–	0.16	Bal.
2¼ Cr1Mo (BS 1501-622)	0.13–0.18	–	0.40–0.80	–	–	2–2.5	0.90–1.20	–	–	–	–	–	–	–	0.30	Bal.
Al (BS 1472)	–	0.5–1.3	0.5	–	–	–	–	–	0.6–1.4	0.2	1.8–2.8	0.2	–	Bal.	0.6–1.4	0.6–1.2
IN-100 (BS)	0.18	0.2	0.2	–	–	9.5–10.5	2.75–3.50	–	–	5.0	0.2	–	15.0	5.5	Bal.	0.5

TABLE II Thermal treatment and Young's modulus of the materials

| Material	Thermal treatment	Young's modulus
X 6 CrNiMo 17 13 (DIN 17006)	Annealing: 1050 °C Permanence: 30 min Cooling: air	In 650 °C range: ∼150 000 MPa
800H (ASTM B163)	Annealing: 950 °C Permanence: 30 min Cooling: water	In 800 °C range: ∼140 000 MPa
10 CrMo 9 10 (DIN 17006)	Annealing: 1150 °C for grain size ASTM 2½	In 650 °C range: ∼140 000 MPa
2¼ Cr1Mo (BS 1501-622)	Annealing for normalization: 940 °C Heating: 695 °C (BS3604-1972)	In 650 °C range: ∼140 000 MPa
Al (BS 1472)	Annealing: 420 °C Under a control slow cooling	In 200 °C range: ∼60 000 MPa
IN-100 (BS)		In 900 °C range: ∼160 000 MPa
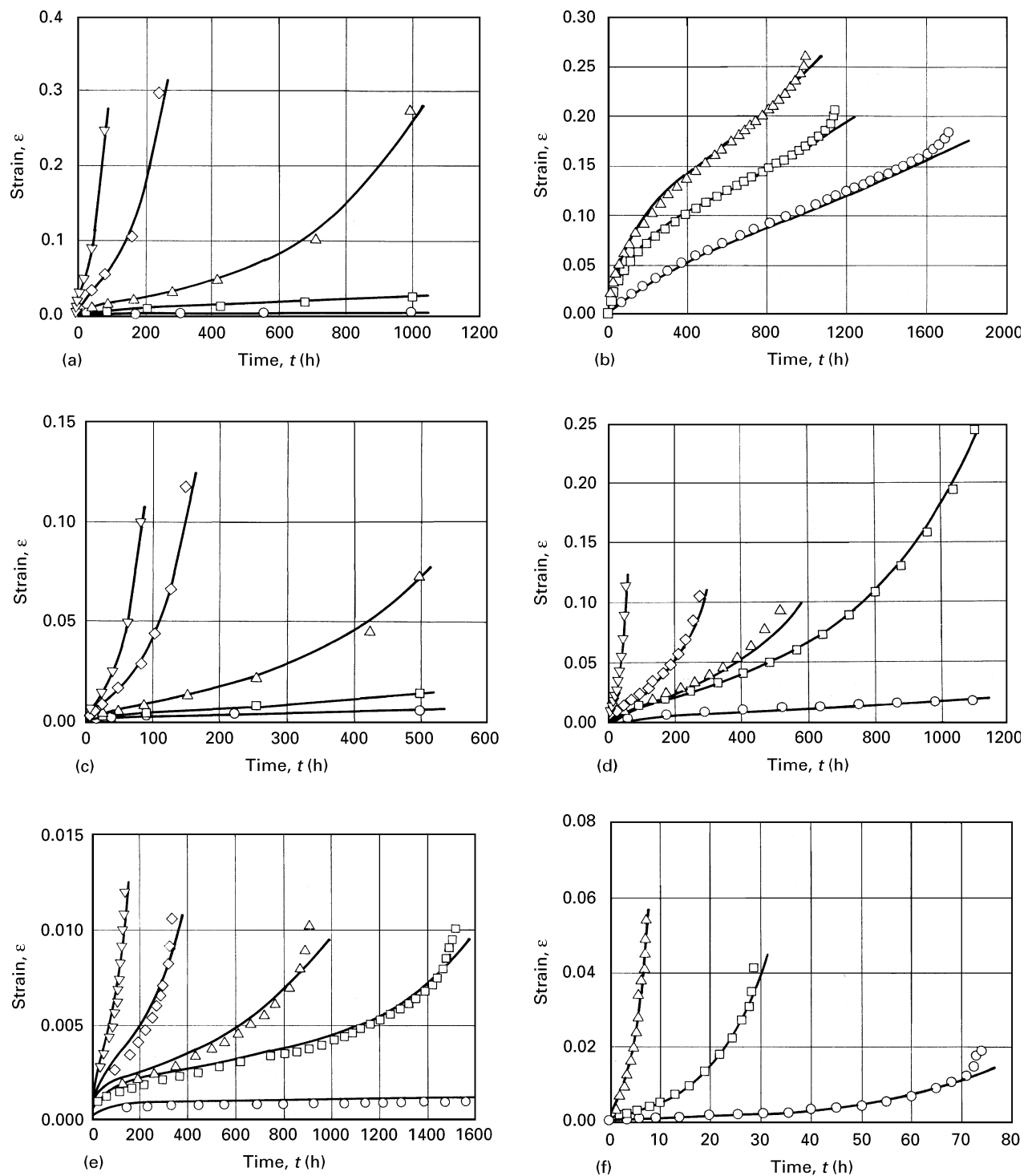
Figure 1 Fitting of the creep strain function (Equation 75) to the experimental data for different metallic materials. (a) X6 CrNiMo 17 13, $T = 973$K. (O) 62 MPa, (□) 78 MPa, (△) 98 MPa, (◇) 123 MPa, (▽) 137 MPa. (——) Fitting; [93]. (b) 800H. $T = 1123$K. (O) 36 MPa, (□) 40 MPa, (△) 43 MPa. (——) Fitting; [80]. (c) 10 CrMo .9 10.$T = 873$K. (O) 62 MPa, (□) 78 MPa, (△) 98 MPa, (◇) 123 MPa, (▽) 137 MPa. (——) Fitting; [93]. (d) $2\frac{1}{4}$ Cr1Mo. $T = 823$K. (O) 155 MPa, (□) 180 MPa, (△) 190 MPa, (◇) 200 MPa, (▽) 230 MPa. (——) Fitting; [80]. (e) Al. $T = 483$K. (O) 34.48 MPa, (□) 51.71 MPa, (△) 55.16 MPa, (◇) 62.06 MPa, (▽) 68.95 MPa. (——) Fitting; [94]. (f) IN 100. $T = 1273$K. (O) 137 MPa, (□) 171 MPa, (△) 205.5 MPa. (——) Fitting; [95, 96].

time. This important fact clearly confirms the correctness of the association of parameters K^* and η^* with the structure of the material.

Generally the coefficients k, l, m, n, p, q depend on the temperature T, that is, are temperature parameters. In a previous study [5], the effect of temperature is incorporated. Then, Equations 80–82 take the following simple forms

$$K(\sigma, T) = k \exp(l_2\sigma - l_1\sigma T) \tag{83}$$

$$\eta(\sigma, T) = m \exp(n_2\sigma - n_1\sigma T) \tag{84}$$

$$\alpha(\sigma, T) = p_1 \exp(q_2\sigma - q_1\sigma T + p_2 T) \tag{85}$$

2521
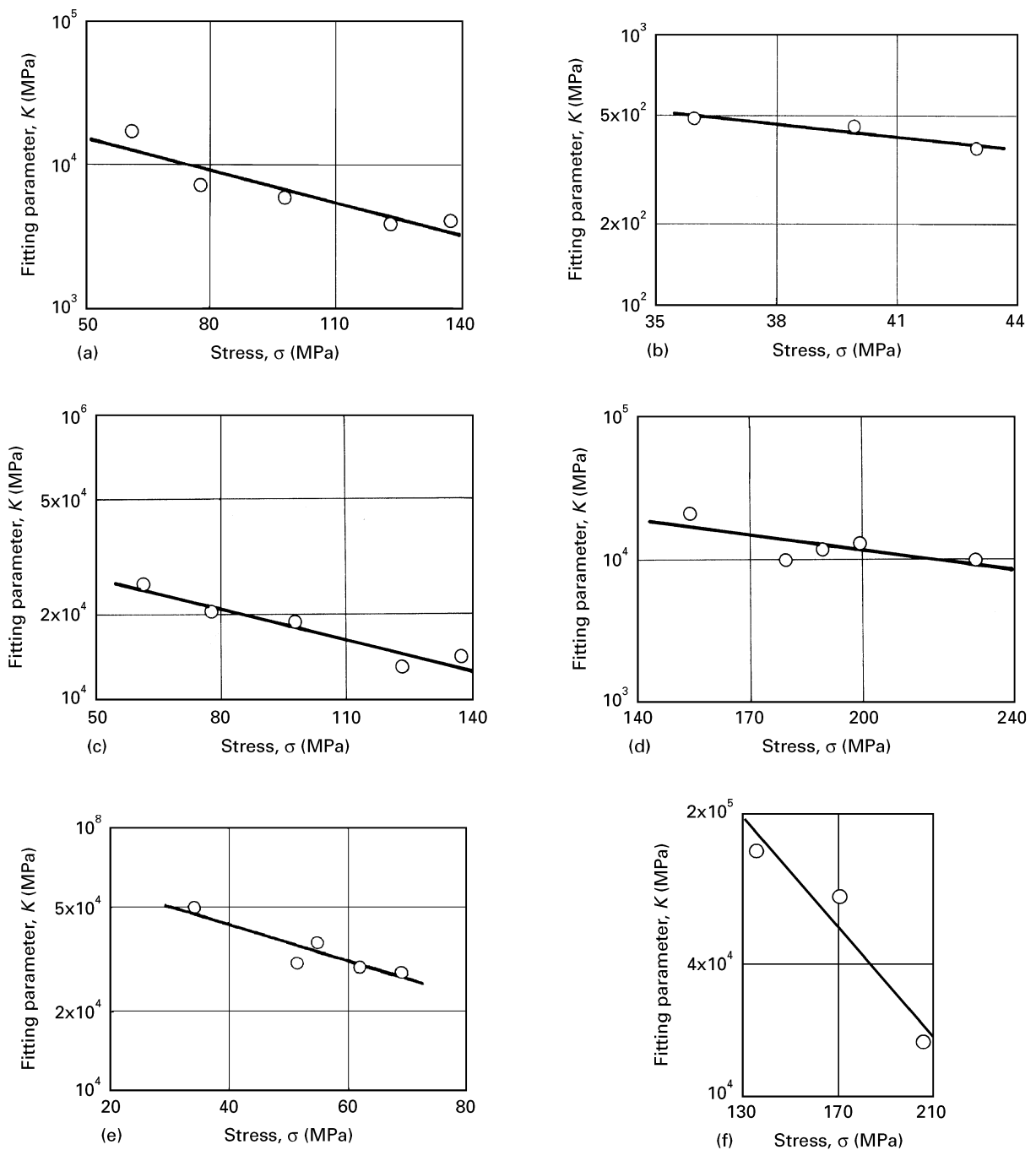
Figure 2 Dependence of the fitting parameter K on the stress for different metallic materials. (a) X6 CrNiMo 17 13, $T = 973K$. (b) 800H, $T = 1123K$. (c) 10 CrMo 9 10, $T = 873K$. (d) $2\frac{1}{4}$ Cr1Mo, $T = 823K$. (e)Al, $T = 483K$. (f) IN 100, $T = 1273K$.

The constants l_1, l_2, n_1, n_2, p_1, p_2, q_1, q_2, k and m are independent of σ and T while they are only dependent on the material and the preceding thermal treatment. That is, there are only ten material constants, a number smaller than in any other relation proposed up to now (16 in the θ-projection equation).

7. Predictions

The linearity of relations $\ln K$–σ, $\ln\eta$–σ, and $\ln\alpha$–σ, as well as the very small deviation of the points from their approximated function, as shown in the Figs 2–4, offers a new, relatively simple, method for the prediction of creep data as well as for the interpolation and extrapolation of experimental data.

For any desired stress, Equations 75, 80–82 and Table II can, essentially, be used in order to construct the predicted creep curve. The method allows for the dependence of the form of the creep curves on the stress to be accurately described in terms of the parameters. If Equations 80–82 are compared to the non-rational dependence of $\hat{n}$ on σ, the result is that the system of the above equations clearly constitutes a rationalization of the creep curve's dependence on the stress. The method offers an appropriate basis for the interpolation and extrapolation of strain data and is ideally compatible with the modern designing methods because the constitutive equation, which exactly describes the behaviour of the material in the stress field, can be used in a computer, a possibility that does not exist with $\hat{n}$ of Equation 54.
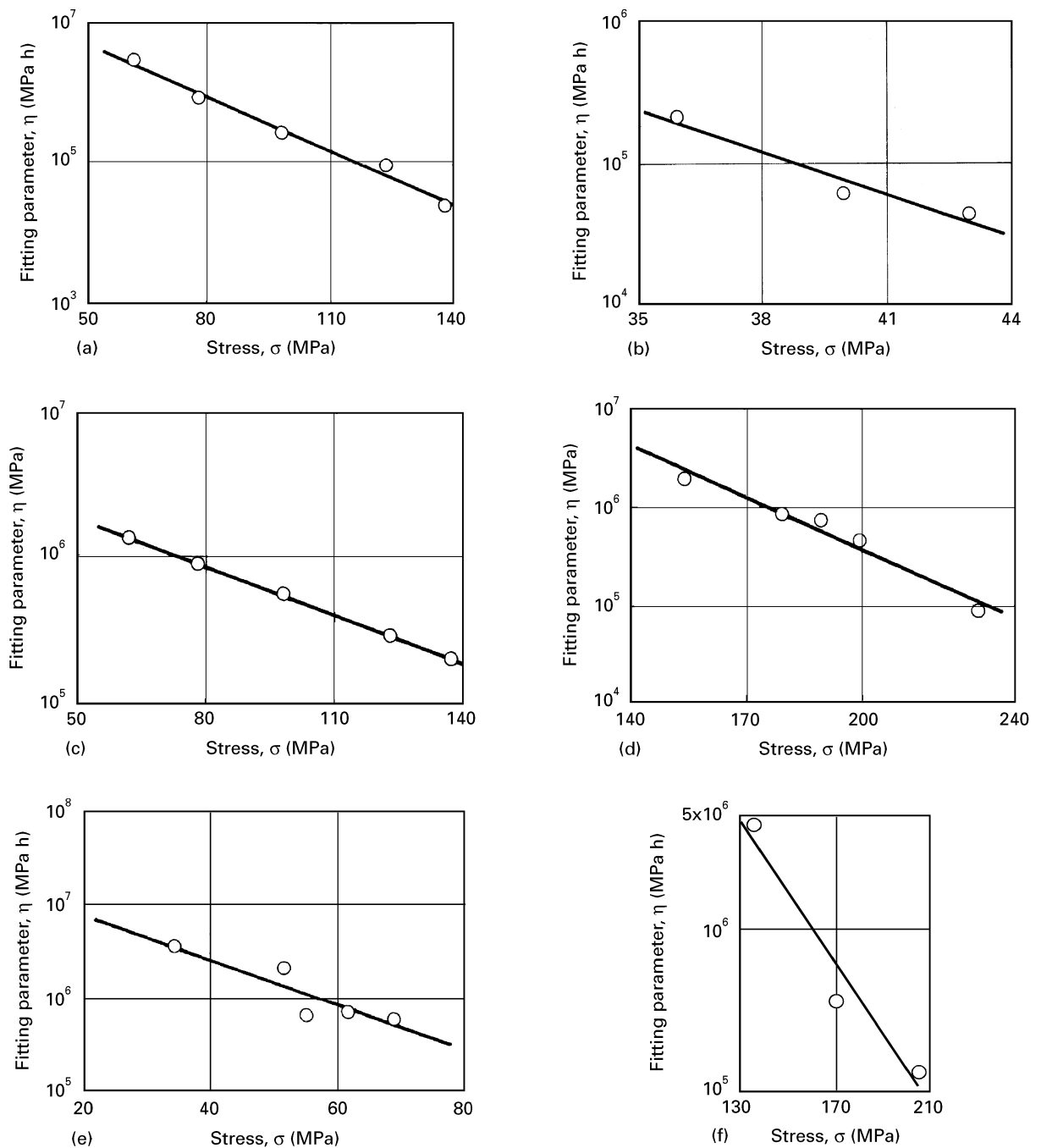
Figure 3 Dependence of the fitting parameter η on the stress for different metallic materials. (a–f) As in Fig. 3.

Fig. 7 shows the predictions produced by the new method. As derived from the figure, there is an excellent predictive capability of the proposed creep function. The same predictive capability exactly results from the tested materials in the laboratory. In Fig. 8 a comparison is made between the predictions of creep function (Equation 75) and the predictions of the creep function of the θ-projection method which, as already mentioned, has the same form but also an additional fitting parameter. The predictions of the θ-projection method were reproduced from other work [80]. The statistical errors in the determination of the fitting parameters operate accumulatively in the creep function. Therefore, the smaller the number of fitting parameters, the smaller are the deviations of the predictions from the experimental data.

8. Conclusion

A physical–phenomenological model for the description of the metallic material creep behaviour has been presented. The model is very general. On the one hand, it is referred to all three stages of creep and, on the other hand, it does not distinguish metallic materials strongly hardened with second-phase particles (precipitation, particle dispersions). The model uses two structure parameters, the derivative of the internal stress and the damage. These parameters correspond to the dominant physical procedures of the dislocations movement and of the cavities development. The basic constitutive equation (as well as the structure parameters) was not arbitrarily formulated but it was derived from an extended and attentive mathematical analysis that reliably represents the dominant physical
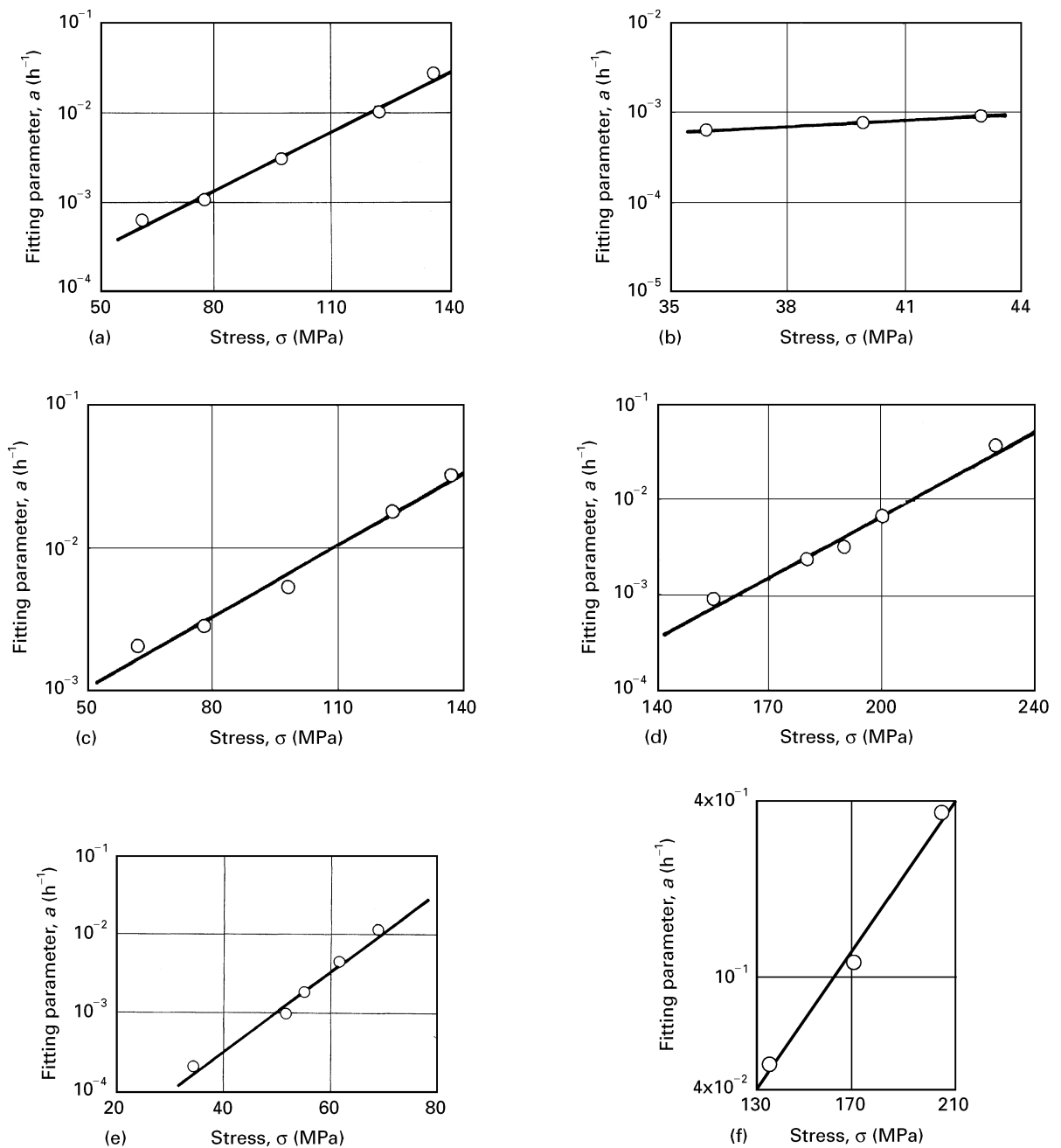
Figure 4 Dependence of the fitting parameter α on the stress for different metallic materials. (a–f) As in Fig. 3.

TABLE III Values of constants of Equations 80–82

Material	Temperature (°C)	k (MPa)	l (MPa^{-1})	m (MPa h)	n (MPa^{-1})	p (h^{-1})	q (MPa^{-1})
X 6 CrNiNo 17 13	700	5.35×10^5	1.67×10^{-2}	8.329×10^7	5.684×10^{-2}	2.489×10^{-5}	4.93×10^{-2}
800 H	850	1.716×10^3	3.429×10^{-2}	7.503×10^8	2.296×10^{-1}	1.14×10^{-4}	4.724×10^{-2}
10 CrMo 9 10	600	4.08×10^4	8.253×10^{-3}	5.780×10^6	2.381×10^{-2}	1.67×10^{-4}	3.759×10^{-2}
$2\frac{1}{4}$ Cr1Mo	500	5.916×10^4	8.003×10^{-3}	1.148×10^9	4.137×10^{-2}	5.085×10^{-7}	5.089×10^{-2}
Al	210	8.174×10^4	1.613×10^{-2}	2.278×10^7	5.389×10^{-2}	3.229×10^{-6}	1.159×10^{-1}
IN-100	1000	9.244×10^6	2.959×10^{-2}	3.796×10^9	5.048×10^{-2}	8.907×10^{-4}	2.893×10^{-2}

procedures at every stage of creep. The descriptive/predictive capability of the produced creep function is due to the solid physical basis of the development of the physical–phenomenological model and to its mathematical processing, which led to minimization in the number of fitting parameters to a number smaller than in any other relation proposed up to now for the description of the entire metallic materials creep curve. The constitutive equation has a particularly simple mathematical form. The new method is

considered to offer a basis for the development of a unified approach to the description of a creep curve which will solve, on the one hand, theoretical problems of the scientists interested in accurate predictions of creep curves and, on the other hand, practical problems of the engineers interested in the accuracy of the constitutive equations in the design concerning metallic materials under high temperatures.
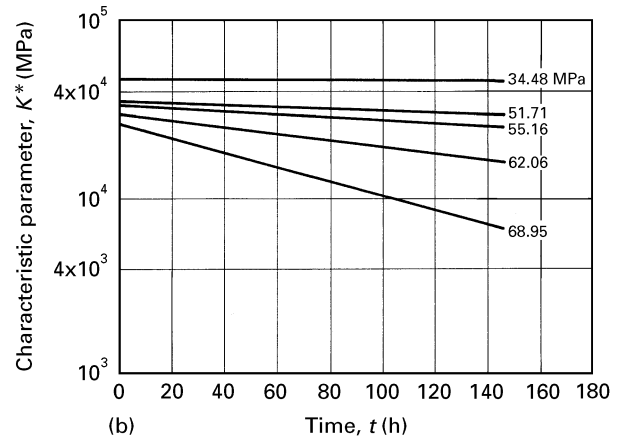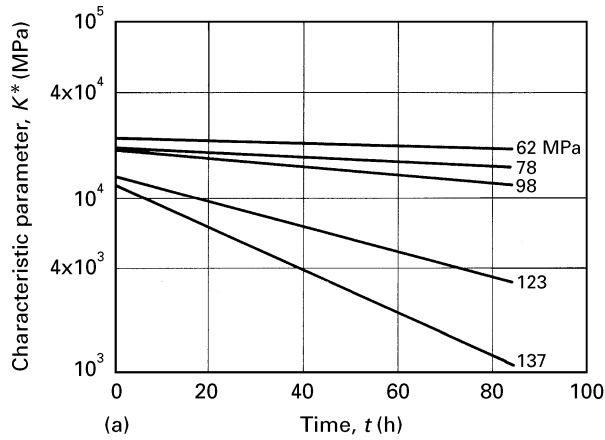

Figure 5 Dependence of the model characteristic parameter K^* on time and for different stresses, for materials (a) 10 CrMo 9 10 at 873K, and (b) aluminium at 483K.
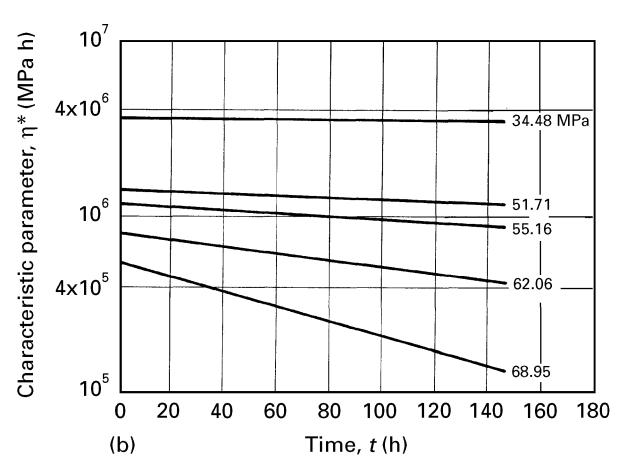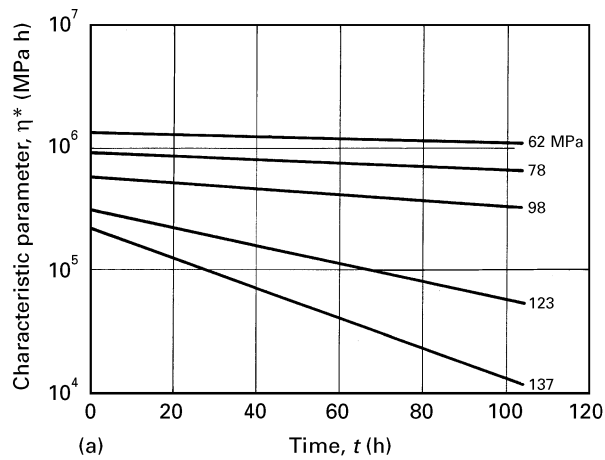
Figure 6 Dependence of the model characteristic parameter η^* on time and for different stresses, for materials (a) 10 CrMo 9 10 at 873K, and (b) aluminium at 483K.
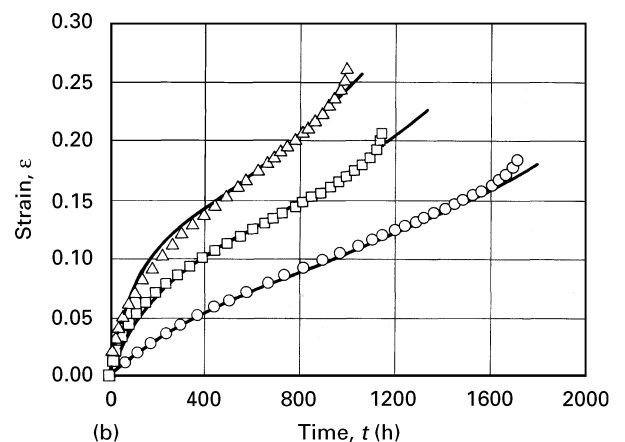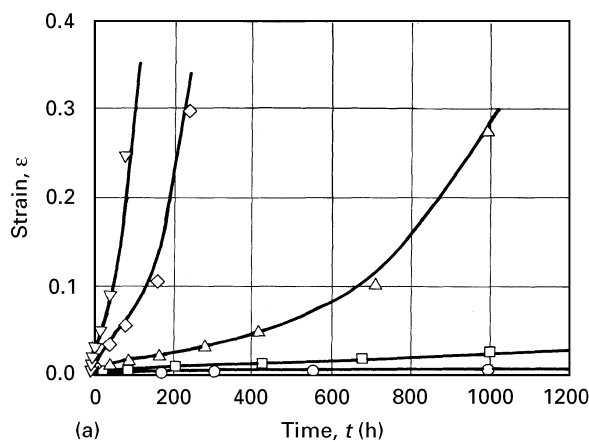
Figure 7 Predictions of creep strain on the basis of Equations 75, 80–82, and Table III for different metallic materials. For key, see Fig. 1, except (——) prediction.
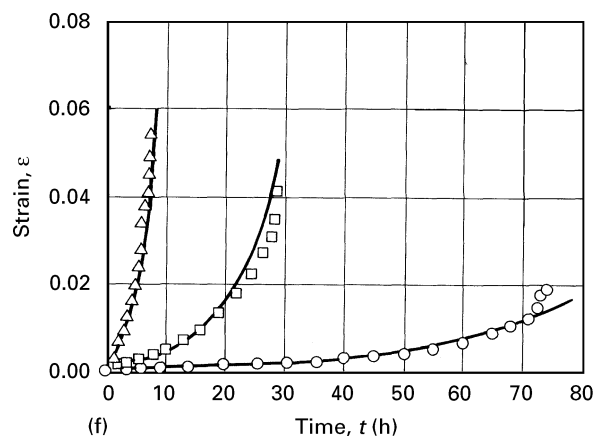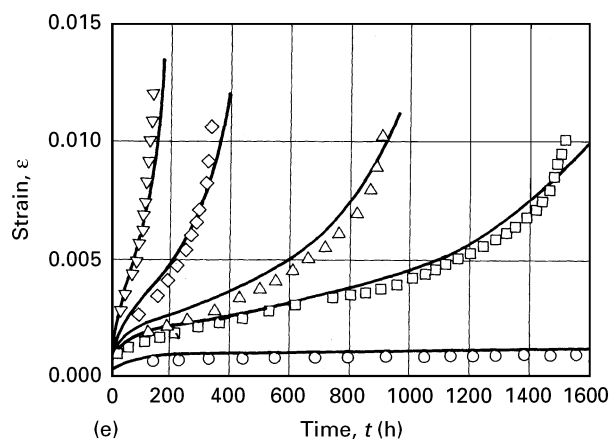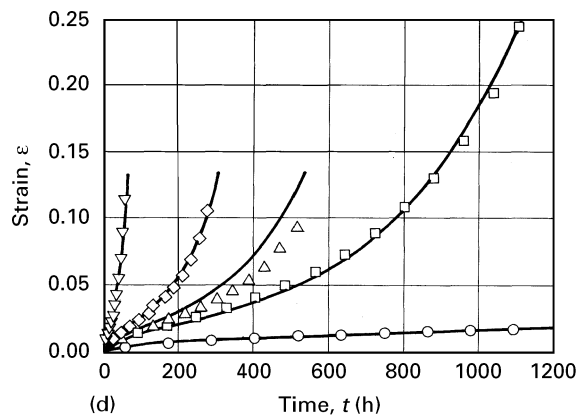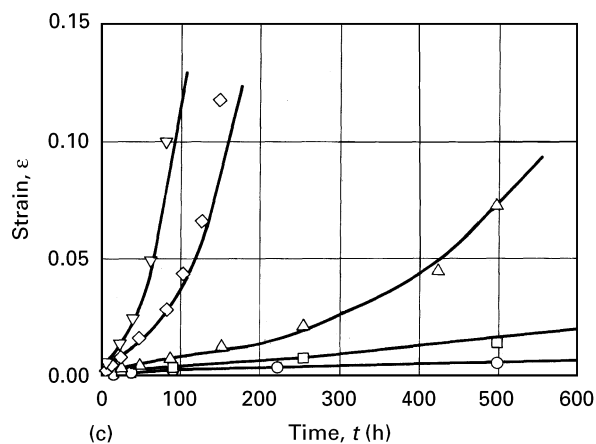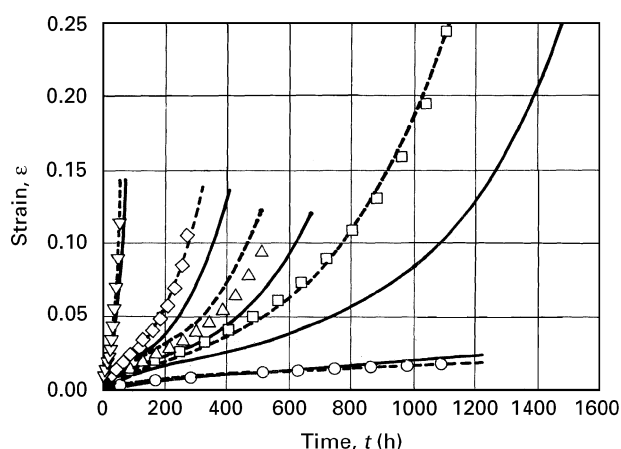
Figure 7 Continued

Figure 8 Comparison of (-----) present model prediction to (——) the predictions of θ-projection method for material $2\frac{1}{4}$ Cr1Mo, at 823 K. (○) 155 MPa, (□) 180 MPa, (△) 190 MPa, (◇) 200 MPa, (▽) 230 MPa.

References

1. T. B. KERMANIDIS, S. G. PANTELAKIS and N. D. BATSOULAS, *Metall.* **31** (1990) 1167.
2. S. G. PANTELAKIS, N. D. BATSOULAS and T. B. KERMANIDIS, *Steel Res.* **62** (1991) 272.
3. S. G. PANTELAKIS, T. KERMANIDIS and N. BATSOULAS, in "Proceedings of the 5th Cairo University MDP Conference" edited by I. Fawzy and M. A. Shirlaby, Cairo, Egypt (Cairo Univ., 1991) p. 23.
4. T. B. KERMANIDIS, S. G. PANTELAKIS and N. D. BATSOULAS, *Theor. Appl. Fract. Mech.* **17** (1992) 7.
5. N. D. BATSOULAS, *Steel Res.* **65** (1994) 114.
6. *Idem, ibid.* **65** (1994) 163.
7. E. OROWAN, *J. W. Scotland Iron Steel Inst.* **54** (1946) 45.
8. N. J. FROST and M. F. ASHBY, Division of Engineering and Applied Science, Harvard University, Internal report (1972).
9. D. J. LOOYD and J. D. EMBORY, *Metall. Sci. J.* **4** (1970) 6.
10. C. N. AHLQUIST, R. CASCA-NERI and W. D. NIX, *Acta Metall.* **19** (1970) 663.
11. C. N. AHLQUIST and W. D. NIX, *ibid.* **19** (1971) 373.
12. A. ORLOVA, M. PAHUTOVA and J. CADEK, *Philos. Mag.* **25** (1972) 865.
13. C. J. BOLTON, "Internal stress: a review with special reference to high temperature creep", Berkeley Nuclear Laboratories, UK, RD/N2300 (1973).
14. J. C. GIBELING and W. D. NIX, *Mater. Sci. Eng.* **11** (1977) 453.
15. M. A. ABDOU, in "Proceedings of the 1st Cairo University MDP Conference" edited by I. Fawzy, Cairo, Egypt (Cairo Univ., 1979) p. 13.
16. M. A. MORRIS and J. L. MARTIN, *Acta Metall.* **32** (1984) 1609.
17. E. EL-MAGD and T. KAISER, in "Proceedings of the 3rd International Conference on Creep and Fatigue" edited by B. Wilshire and D. R. J. Owen (Institute of Metals, London, 1987) p. 130.
18. E. EL-MAGD and A. D. MEGAHED, in "Proceedings of the 4th Cairo University MDP Conference" edited by M. M. Megahed, Cairo, Egypt, (Cairo Univ., 1988) p. 35.
19. E. EL-MAGD and C. SHAKER, in "Proceedings of the 4th International Conference on Creep and Fracture of Engineering Materials and Structures" edited by B. Wilshire and R. Evans (Institute of Metals, London 1990) p. 119.
20. J. WEERTMAN, *Acta Metall.* **25** (1977) 1393.
21. J. J. JONAS, *ibid.* **17** (1969) 1393.
22. A. A. SOLOMON and W. D. NIX, *ibid.* **18** (1970) 863.
23. F. DODES and F. CADEK, *Phys. Status Solidi (a)* **35** (1976) 123.
24. P. FELTHAM, *ibid.* **30** (1968) 135.
25. *Idem, J. Phys.* **D6** (1973) 2048.

26. J. H. GITTUS, *J. Mech. Phys. Solids* **13** (1965) 69.
27. G. SAADA, in "Electron Microscopy and Strength of Crystals", edited by G. Thomas and J. Washburn (Interscience, New York, 1963) p. 53.
28. R. LAGNEBORG, B. H. FORSEN and J. WIBERY, "Creep Strength in Steel and High Temperature Alloys" (The Metals Society, London, 1974).
29. F. DOBES, *Acta Metall.* **28** (1980) 377.
30. R. K. HAM, *Philos. Mag.* **6** (1961) 1183.
31. A. ORLOVA, *Scripta Metall.* **16** (1982) 633.
32. E. OROWAN, *Proc. Phys. Soc.* **52** (1940) 8.
33. *Idem, Nature* **149** (1942) 643.
34. U. F. KOCKS, *ASME J. Eng. Mater. Tech.* **98** (1976) 76.
35. M. BRAUM, "Differential Equations and their Applications" (Springer, New York, 1978).
36. J. HALE, "Studies in Ordinary Differential Equations" (Mathematical Association of America, New York, 1977).
37. B. F. DYSON and M. McLEAN, *Acta Metall.* **31** (1983) 17.
38. G. GREENWOOD, *Philos. Mag.* **17** (1978) 423.
39. *Idem*, in "Proceedings of the International Congress on Metals", Cambridge (The Metals Society, Cambridge, 1973) p. 91
40. B. F. DYSON and D. McLEAN, *Metal Sci. J.* **2** (1977) 37.
41. Y. N. RABOTNOV, "Creep Problems in Structural Members" (North-Holland, Amsterdam, 1969).
42. M. RIDES, A. C. COCKS and D. R. HAYHURST, *ASME J. Appl. Mech.* 56 (1989) 493.
43. E. EL-MAGD, S. PANTELAKIS and K. JAGER, *Res. Mech.* **21** (1987) 55.
44. F. A. LECKIE, *Eng. Fract. Mech.* **25** (1986) 501.
45. F. A. LECKIE and D. R. HAYHURST, *Acta Metall.* **25** (1977) 1059.
46. L. M. KACHANOV, "Theory of Creep" (Boston Spa, Wetherby, 1960).
47. *Idem*, in "Problems of Continuum Mechanics, Contributions in Honor of 70th Birthday of N. I. Muskhelishvili", edited by J. R. M. Radok, (Society for Industrial and Applied Mathematics, Philadelphia, PA, 1961) p. 100.
48. P. W. DAVIES and P. W. EVANS, *Acta Metall.* **13** (1965) 353.
49. P. W. DAVIES and R. DUTTON, *ibid.* **15** (1967) 1365.
50. M. R. SITZER and A. TROOST, *Z. Werkstofftech.* **15** (1984) 264.
51. A. TROOST, *ibid.* **14** (1983) 336.
52. J. MARIN, *Proc. SESA* **11** (1970) 207.
53. Y. ESTRIN and H. MECKING, *Acta Metall.* **32** (1984) 57.
54. W. V. GREEN, in "Techniques of Metals Research", edited by R. F. Bunsaw, (Interscience, New York, 1971) p. 39.
55. R. LAGNEBORG, in "Creep and Fatigue in High Temperature Alloys" edited by J. Bressers (Applied Science, London, 1980) p. 41.
56. K. R. WILLIAMS and B. WILSHIRE, *Mater. Sci. Eng.* **47** (1981) 151.
57. A. J. KENNEDY, "Processes of Creep and Fatigue in Metals" (Wiley, New York, 1963).
58. B. C. HOSKIN, "Phenomenological Theories of Time Effects in Metals at High Temperatures with Special Reference to Primary Creep", Brown University, Division of Engineering Research, 562(20)/7 (1958).
59. S. BHATTACHARYA, *J. Inst. Metals* **81** (1952–1953) 83.
60. A. H. COTTREL, *J. Mech. Phys. Solids* **1** (1952) 53.
61. J. MARIN, *Proc. SESA* **11** (1970) 207.
62. A. D. SCHWOPE and L. R. JACKSON, "A Survey of Creep in Metals", NACA TN 2516 (1951).
63. A. E. JOHNSON and A. E. FROST, *J. Inst. Metals* **81** (1952–53) 93.
64. F. GAROFALO, *ASME J. Basic. Eng.* **82** (1960) 867.
65. Y. H. PAO and J. MARIN, *ASME J. Appl. Mech.* **20** (1953) 245.
66. Y. N. RABOTNOV, "Some Problems of the Theory of Creep" (translation), NACA TN 13567 (1953).
67. K. SCHAAR, *Materialprufung* **6** (1964) 130.
68. C. E. PUGH, in "Advances in Design for Elevated Temperature Environment", edited by S. Y. Zamrik and R. J. Jeffer (ASME, New York, 1975) p. 137.
69. O. D. SHERBY and J. WADSWORTH, "Deformation, Processing and Structure", (ASM, Metals Park, OH, 1984).
70. P. W. DAVIES and R. DUTTON, *Acta Metall.* **15** (1967) 1365.
71. P. W. DAVIES and K. R. WILLIAMS, *ibid.* **17** (1969) 897.
72. A. GRAHAM and F. K. A. WALLES, *J. Iron Steel Inst.* **193** (1955) 105.
73. R. W. EVANS, J. P. PARKER and B. WILSHIRE, in "Recent Advances in Creep and Fracture of Engineering Materials and Structures", edited by B. Wilshire and D. R. J. Owen, (Pinieridge Press, Swansea, 1982) p.135.
74. B. WILSHIRE and D. R. J. OWEN, "Engineering Approaches to High Temperature Design", (Pineridge Press, Swansea, 1983).
75. R. W. EVANS, I. BEDEN and B. WILSHIRE, in "Proceedings of the 2nd International Conference on Creep and Fracture of Engineering Materials and Structures" (Pineridge Press, Swansea, 1984) p. 1277.
76. R. W. EVANS and B. WILSHIRE, "Creep of Metals and Alloys" (Institute of Metals, London, 1985).
77. N. CHRISTODOULOU, *Scripta Metall.* **20** (1986) 1041.
78. S. L. SEMIATIN, A. K. GHOSH and J. J. JONAS, *Metall. Trans.* **16A** (1985) 2291.
79. J. LEMAITRE and J. L. CHABOCHE, "Mechanics of Solids Materials" edited by Engins (Cambridge University Press, London, 1990).
80. N. TAYLOR, B. TWADDLE and R. C. HURST, in "Proceedings of the 4th International Conference on Creep and Fracture of Engineering Materials and Structures" edited by B. Wilshire and R. Evans (Institute of Metals, London, 1990) p. 985.
81. F. GAROFALO, "Fundamentals of Creep and Creep-rupture in Metals" (Macmillan, New York, 1965).
82. R. H. ERICKSEN and G. J. JONES, *Metall. Trans.* **3A** (1972) 1735.
83. O. D. SHERBY, T. A. TROZERA and J. E. DORN, *Proc. ASTM* **56** (1956) 784.
84. D. MCLEAN and K. F. HALE, in "Proceedings of the Symposim on Structural Processes in Creep" (Iron and Steel Institute, London, 1961) p. 19.
85. P. FELTHAM and J. D. MEAKIN, *Acta Metall.* **7** (1959) 614.
86. E. R. PARKER, *Trans. ASM* **50** (1958) 85.
87. L. RAYMOND and J. E. DORN, *ibid.* **230** (1964) 560.
88. G. BRINSON and B. ARGENT, *J. Inst. Metals* **91** (1963) 293.
89. R. P. CARREKAR, *J. Appl. Phys.* **21** (1950) 1289.
90. W. J. EVANS and B. WILSHIRE, *Met. Sci. J.* **4** (1970) 89.
91. D. SIDEY and B. WILSHIRE, *ibid.* **3** (1969) 56.
92. K. E. AMIN, A. K. MUKHERJEE and J. E. DORN, *J. Mech. Phys. Solids* **18** (1970) 413.
93. H. BARTH, Dr -Ing Dlss, Thecnischen Hochschule Darmstadt, Darmstadt (1984).
94. D. R. HAYHURST, P. R. DIMMER and M. W. CHERNUKA, *J. Mech. Phys. Solids* **23** (1975) 333.
95. J. L. CHAHOCHE, "Description thermodynamique et phenomenologiique de la viscoplasticite cyclique avec endommagement", (ONERA, Paris, 1978).
96. D. KRAJCINOVIC and S. SELVARAJ, *ASME J. Eng. Mater. Technol.* **106** (1984) 405.